PAPER

Novel triarylamine-based aromatic polyamides bearing secondary amines: synthesis and redox potential inversion characteristics induced by pyridines†

Hung-Ju Yen,‡§[a] Jhe-Huang Lin,‡[a] Yuhlong Oliver Su*[b] and Guey-Sheng Liou*[a]

Novel triarylamine-based aramids with secondary amine moieties are prepared and utilized as electrochemical detectors for pyridines. Their electrochemical behavior with different pyridines was investigated in order to demonstrate the ionic hydrogen bonding interaction of the secondary amine with the pyridines, resulting in obvious potential inversion which is also supported by *in situ* absorption measurements.

Introduction

Recently, polymers with molecular recognition sites have become highly attractive and are considered to be sensitive chemosensors because of their notable electronic and optical properties,[1] making them particularly suited to these applications. Their high sensitivity originates from the conformation changes and difference in electron distribution of the polymer main-chain caused by the interaction between the recognition site and the target. Consequently, the absorption, fluorescence, conductivity, or redox potential of the polymer changes. Nowadays, detectors with high sensitivity and reliability are urgently required due to the degenerating environment and the increasing risk of chemical and biological threats. In particular, significant efforts have been made to seek new chemosensory systems for materials which have the potential to cause harm to humans, animals, or the environment, either by themselves or through interaction with other factors.

Pyridine and its derivatives are key chemicals as solvents and intermediates for the production of agricultural chemicals, additives, dyes, drugs, *etc.* However, these toxic and foul-smelling substances intrude into the human living environment through exhaust gases and various industrial wastes. These chemicals can cause acute effects on the human body when ingested, inhaled, or absorbed through the skin, including vomiting, nausea, coughing, asthmatic breathing, headaches, and even cancers. In addition, pyridine may also have minor neurotoxic, genotoxic, and clastogenic effects. Therefore, the development of detectors for harmful pyridines is in high demand for human health and an eco-friendly society.

Notably, some important works done by Linschitz[2] and Smith[3] elucidated the interactions between the reduced compounds and hydrogen donors, such as alcohols, amides and ureas, which can be monitored by CV. In addition, Su's group[4] synthesized a series of phenylenediamines that could form hydrogen bonds with pyridines or alcohols, and the potential shift exhibited a different CV pattern on the oxidative aspect. The process of potential shift could be classified as potential inversion with a single two-electron wave, which is rare and mostly observed when significant structural change,[5] large solvation[6] or redox potentials by ionic hydrogen bonding[2] occurred within the multi-electron transfer reaction. Nevertheless, these compounds are very rare.

Therefore, in this work we introduced a new polymeric chemosensor with potential inversion characteristics, which is designed for the sensing of pyridines *via* changes in electrochemistry and optical absorption. Triphenylamine-based polymers with secondary amines were chosen and synthesized due to their well-known photo- and electroactive properties and featured ionic hydrogen-bonding abilities with pyridines. These target polymers exhibit several advantages: facile preparation by the polycondensation of a diamine monomer with various commercial compounds, high thermal stability, and the ability to interact with pyridines accompanied by potential inversion and intense absorption changes originating from ionic hydrogen bonding.

[a] *Institute of Polymer Science and Engineering, National Taiwan University, 1 Roosevelt Road, 4th Sec., Taipei 10617, Taiwan. E-mail: gsliou@ntu.edu.tw*

[b] *Department of Applied Chemistry, National Chi Nan University, Puli, Nantou 54561, Taiwan. E-mail: yosu@ncnu.edu.tw*

‡ H. J. Yen and J. H. Lin contributed equally.

§ Present address: Physical Chemistry and Applied Spectroscopy, Chemistry Division, Los Alamos National Laboratory, Los Alamos, New Mexico 87545, USA.

This journal is © The Royal Society of Chemistry 2016

J. Mater. Chem. C, 2016, **4**, 10381–10385 | **10381**

Results and discussion

Monomer synthesis

Considering the preferential reactivity of the N,N′-diaryl-p-phenylenediamines **1**, the secondary amine attached to the nitrobenzene is more acidic than the one attached to the benzene/methoxybenzene, thus facilitating the deprotonation and subsequent nucleophilic substitution of 4-fluoronitrobenzene. Therefore, N,N-bis(4-nitrophenyl)-N′-phenylbenzene-1,4-diamine (**2-H**) and N-(4-methoxyphenyl)-N′,N′-bis(4-nitrophenyl)benzene-1,4-diamine (**2-OMe**) can be readily prepared through the CsF-mediated aromatic nucleophilic substitution reaction of N-(4-nitrophenyl)-N′-phenyl-1,4-phenylenediamine (**1-H**) and N-(4-methoxyphenyl)-N′-(4-nitrophenyl)benzene-1,4-diamine (**1-OMe**), respectively, with 4-fluoronitrobenzene in high yield (>75%) (Scheme 1). N,N-Bis(4-aminophenyl)-N′-phenyl-benzene-1,4-diamine (**3-H**) and N,N-bis(4-aminophenyl)-N′-(4-methoxyphenyl)benzene-1,4-diamine (**3-OMe**) were then synthesized from dinitro compounds **2** and **2-OMe**, respectively, by Pd/C-catalyzed hydrazine reduction. Elemental analysis, NMR and FT-IR spectroscopic techniques were utilized to confirm the structures of dinitro compounds **2** and target diamine monomers **3**. The FT-IR spectra of these synthesized compounds are illustrated in Fig. S1 and S2 (ESI†). The nitro groups of compounds **2** exhibited two characteristic bands at around 1580 and 1305 cm^{-1} for –NO$_2$ asymmetric and symmetric stretching, respectively. After reduction to diamine monomers **3**, the characteristic absorption bands of the nitro group disappeared and the primary and secondary amino groups showed a typical absorption pair at 3400–3330 cm^{-1}. ^{1}H and ^{13}C NMR, 2D H–H COSY and C–H HSQC NMR spectra of compounds **1–3** are illustrated in Fig. S4–S13 (ESI†), and the results are in perfect agreement with the proposed molecular structures. The model compounds **M** were also prepared by the condensation of diamines **3** with two equivalent amounts of benzoyl chloride for obtaining simplified structural information of their corresponding polyamides (Scheme 2). Their FT-IR and ^{1}H NMR spectra are shown in Fig. S3 and S14 (ESI†), respectively.

Polymer synthesis

Aromatic polyamides (aramids) **PA-H** and **PA-OMe** containing secondary amines with different substituents were prepared by reacting diamines **3-H** and **3-OMe**, respectively, with the commercially available diacid chloride via low-temperature polycondensation (Scheme 3). The polymerization reaction proceeded homogeneously and the high molecular weight
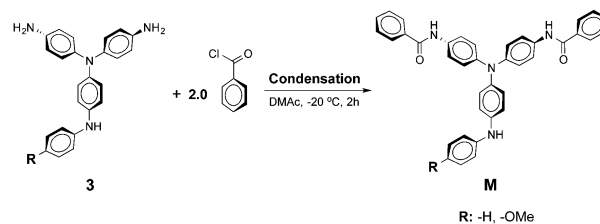
Scheme 2   Synthetic routes to the model compounds.
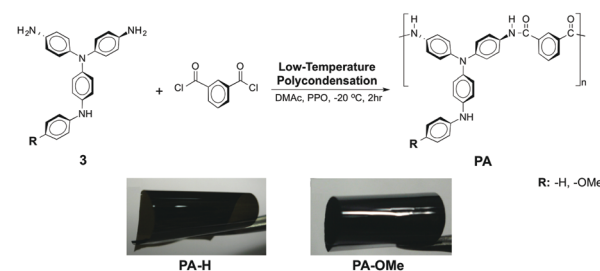
Scheme 3   Synthesis and structure of polyamides **PA-H** and **PA-OMe**.

polymers can afford tough and flexible films via solution casting (as shown in the inset figure of Scheme 3). Due to the strong intra- and inter-chain hydrogen bonding and weak steric hindrance for close packing, the precipitated polyamides showed a relatively low solubility. The precipitated polyamides can only dissolve in H$_2$SO$_4$ with inherent viscosities in the range of 0.95–1.02 dL g^{-1}, indicating the formation of high molecular weight polymers (Table S1, ESI†). Nevertheless, high performance thin films can still be obtained by spin-coating or inkjet-printing of the as-prepared polymer solution without the precipitation/work-up step or using the harmful H$_2$SO$_4$ as a processing solvent.

The IR spectra of the polyamides **PA-H** and **PA-OCH$_3$** shown in Fig. S15 (ESI†) exhibit characteristic absorption bands of the amide group at around 3330 cm^{-1} (amide and secondary N–H stretching) and 1655 cm^{-1} (amide carbonyl). Fig. S16 (ESI†) shows a typical ^{1}H spectrum of **PA-H** in DMSO-d_6; all the peaks could be readily assigned to the hydrogen of the recurring unit. The results identified by IR and NMR spectroscopic techniques demonstrated good agreement with the proposed molecular structures.

Basic polymer properties

The thermal behavior of the obtained polyamides was evaluated by TGA and TMA, and the results are summarized in Table S2
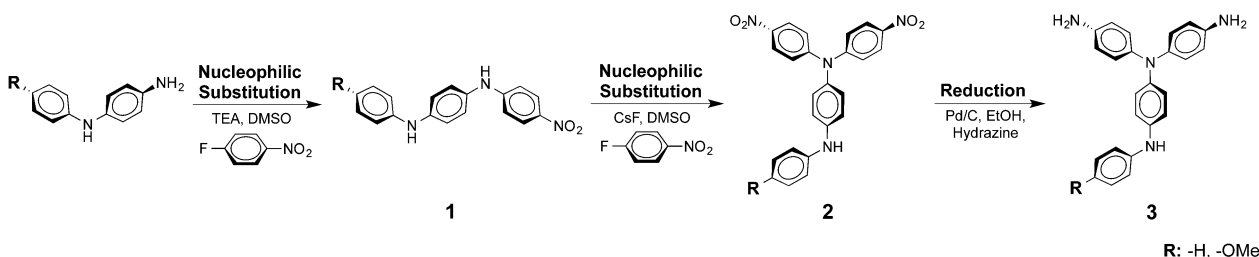
Scheme 1   Synthetic routes to diamine monomers **3-H** and **3-OMe**.

(ESI†). Typical TGA curves of the polyamides are depicted in Fig. S17 (ESI†). All the prepared polymers manifest insignificant weight loss up to 405 °C under nitrogen and air atmosphere, and the carbonized residue (char yield) of these polymers in a nitrogen atmosphere were more than 64% at 800 °C, estimating LOI values up to 44. The softening temperature (T_s) could be easily measured in the TMA thermograms (as shown in Fig. S18, ESI†). The excellent thermal properties indicated that the high aromatic content and strong intra-/inter-chain hydrogen bonding played important roles in the prepared polyamides.

Electrochemistry and *in situ* UV-vis absorption

All of the prepared phenylenediamines reveal two reversible oxidation steps related to the radical cation and dication. The electrochemical behavior of compounds **2**, **3**, and the polyamides were investigated by cyclic voltammetry (CV). The compounds (10 μmol) were dissolved in acetonitrile (CH_3CN) containing 0.1 M tetrabutylammonium perchlorate (TBAP) as an electrolyte and using a glassy carbon disk as the working electrode. In addition, the polymers were conducted by casting a film (polymer films with an area of about 0.5 cm × 1.1 cm) on indium-tin oxide (ITO)-coated glass as the working electrode. As shown in Fig. 1, there are two reversible oxidation redox

couples for compounds **2-H** or **2-OMe** before adding pyridines, which is termed ''normal potential'', indicating that the second oxidation occurs at a higher applied potential than the first one due to electrostatic repulsion. Moreover, as the *para*-substitution changed from a hydrogen atom to an electron-donating methoxy group, compound **2-OMe** ($E_1^{ox} = 0.77$ V; $E_2^{ox} = 1.07$ V) exhibited lower oxidation potentials than that of compound **2-H** ($E_1^{ox} = 0.87$ V; $E_2^{ox} = 1.16$ V) due to the inductive effect of the substituent.

As shown in Fig. 1a–d, after 4-acetylpyridine (AcPy; $pK_a = 3.51$) or pyridine (Py; $pK_a = 5.28$) was added to the solution of nitro-compound **2**, the peak/current of the second oxidation wave was only slightly shifted. Meanwhile, when the more basic 2,4,6-trimethylpyridine (Me₃Py; $pK_a = 7.48$, Fig. 1e and f) was added, a new oxidation wave occurred at a lower potential than the first redox couple (beginning with the red dashed line). The final CV curve (blue solid line) in the presence of 1 equiv. (10.0 μmol) of Me₃Py exhibited only one redox couple at $E_2^{ox'} = 0.81$ and 0.66 V for **2-H** and **2-OMe**, respectively, which are lower values than the normal potential E_1^{ox} of the corresponding **2-H** and **2-OMe**.

Meanwhile, to simplify the structural information of the polyamides, model compounds **M** were prepared and used for
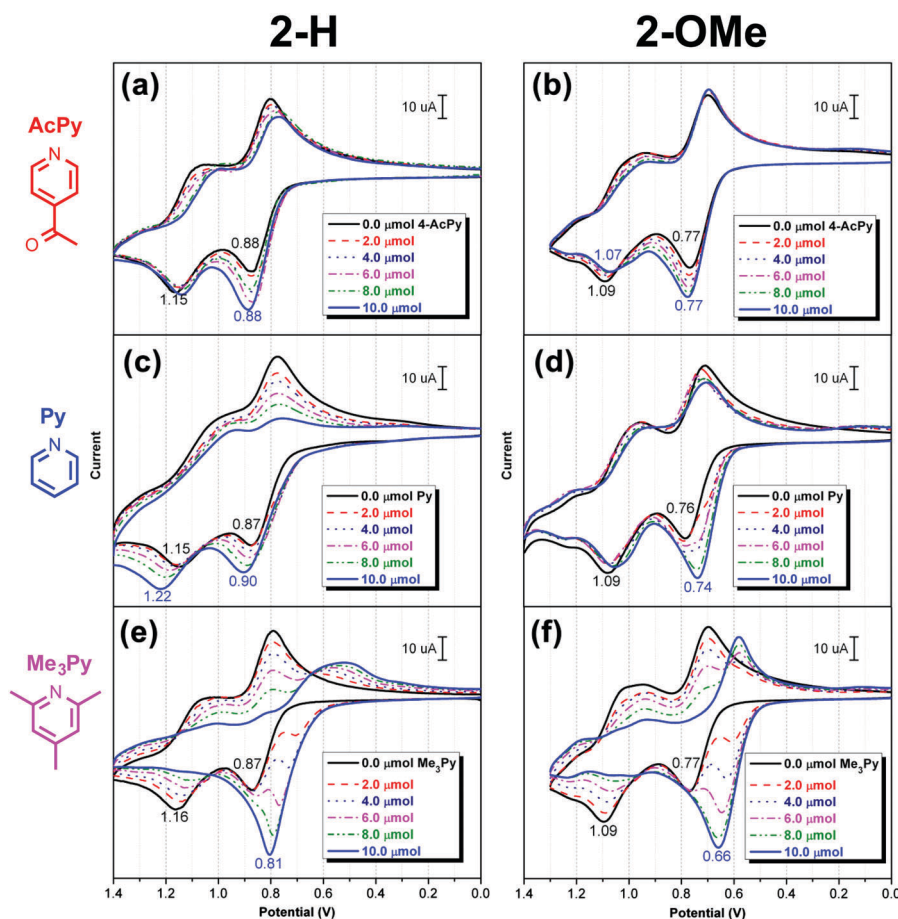

Fig. 1 Cyclic voltammograms of 10 μmol of **2-H** (a, c and e) and **2-OMe** (b, d and f) in 0.1 M TBAP/CH₃CN with various amounts of (a and b) AcPy [$pK_a = 3.51$], (c and d) Py [$pK_a = 5.28$] and (e and f) Me₃Py [$pK_a = 7.48$]. Scan rate: 100 mV s⁻¹. Working electrode: glassy carbon disk (area = 0.07 cm²).
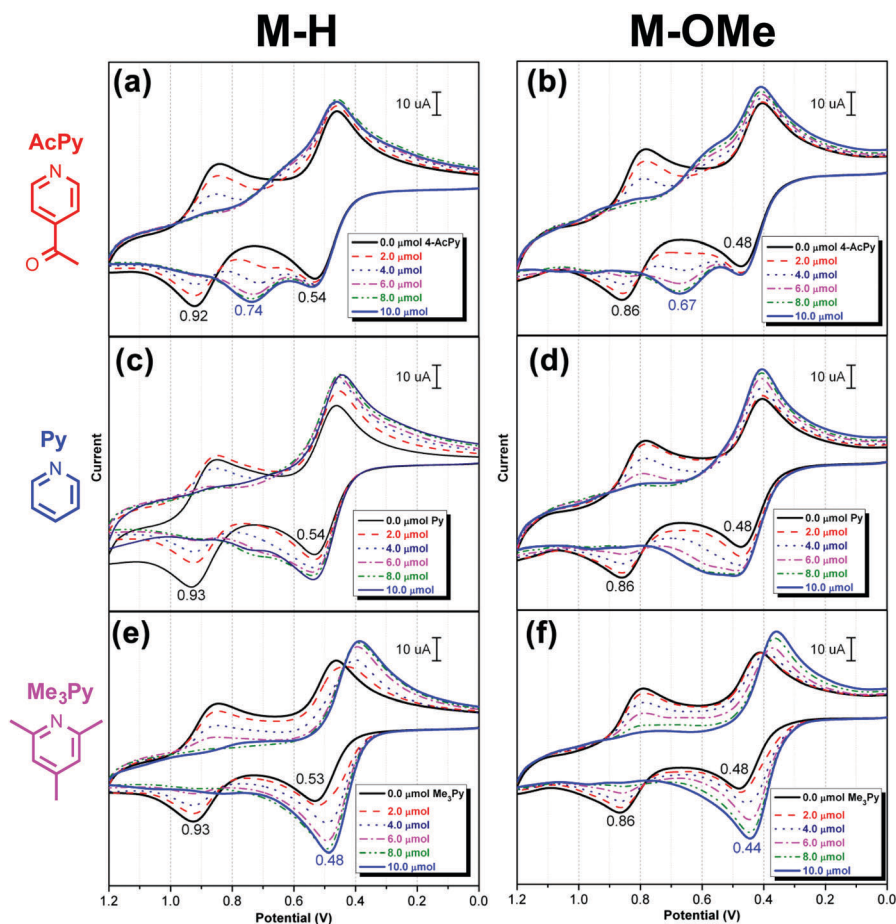
M-H   M-OMe

Fig. 2 Cyclic voltammograms of 10 μmol **M-H** (a, c and e) and **M-OMe** (b, d and f) in 0.1 M TBAP/CH$_3$CN with various amounts of (a and b) AcPy [pK_a = 3.51], (c and d) Py [pK_a = 5.28] and (e and f) Me$_3$Py [pK_a = 7.48]. Scan rate: 100 mV s^{-1}. Working electrode: glassy carbon disk (area = 0.07 cm^2).

CV measurement. As shown in Fig. 2, **M-H** exhibits two reversible redox couples at E_1^{ox} = 0.54 V and E_2^{ox} = 0.92 V, respectively. After AcPy (pK_a = 3.51, Fig. 2a) was added to the solution of **M-H**, a new oxidation wave ($E_2^{ox'}$ = 0.74 V) appeared between E_1^{ox} and E_2^{ox}. The first oxidation remained unchanged, and the current of the second oxidation at E_2^{ox} = 0.92 V gradually decreased on increasing the amount of AcPy. When the amount of AcPy reached 1 equiv. (10.0 μmol) to **M-H**, the second oxidation wave completely disappeared and the appearance of $E_2^{ox'}$ with a lower oxidation potential than E_2^{ox} is assigned as the new second oxidation associated with AcPy. In addition, the addition of Py (pK_a = 5.28; Fig. 2c and d) doesn't shift the E_1^{ox} but further lowered the $E_2^{ox'}$ seeming to merge with E_1^{ox} as the Py concentration reached 1 equiv. (10.0 μmol) of **M**.

Furthermore, when Me$_3$Py (pK_a = 7.48, Fig. 2e) was added to the **M-H** solution, the CV exhibited different patterns to those of AcPy and Py. The new redox wave appeared at a much lower potential than that of E_1^{ox}. The final CV curve (blue solid line of Fig. 2e) with 1 equiv. (10.0 μmol) of Me$_3$Py showed only one redox couple at $E_2^{ox'}$ = 0.48 V, which is apparently lower than E_1^{ox}. Also, the final peak current is about 2 times higher than the first one, indicating that the hydrogen bonding played a

significant role in stabilizing the oxidized product and further favored the second oxidation. As chemosensors require high selectivity and sensitivity to the substrates, we further measured the CVs of model compound **M-OMe** with equal moles of aliphatic amine methylamine and aromatic amine aniline, for comparison (Fig. S19, ESI†). Only the CV curve in the presence of aniline shows a slight shift of the second oxidation potential, which is unobservable when compared with the pyridine derivatives (Fig. 2b, d, and f). In addition, the presence of H-bonding is also supported by UV-vis spectra of **M-OMe**$^{+•}$ after adding Me$_3$Py. The absorption spectra change in Fig. S20 (ESI†) revealed that **M-OMe**$^{+•}$ exhibited a characteristic broad band in the NIR region, which is due to IV-CT excitation between states in which the positive charge was centered at different nitrogen atoms.[7] After Me$_3$Py was added to the solution of **M-OMe**$^{+•}$, the intensity of the absorption peak at 660 nm gradually increased, and a broad band centered at 900 nm in the NIR region gradually decreased in intensity. After adding the equiv. (10.0 μmol) of Me$_3$Py, the complete disappearance of the IV-CT band in the NIR region attributable to the H-bond formation between **M-OMe**$^{+•}$ and Me$_3$Py confirms the phenomenon.

The shift of the second oxidation wave for the model compounds affected by the strength of H-bonding indicates
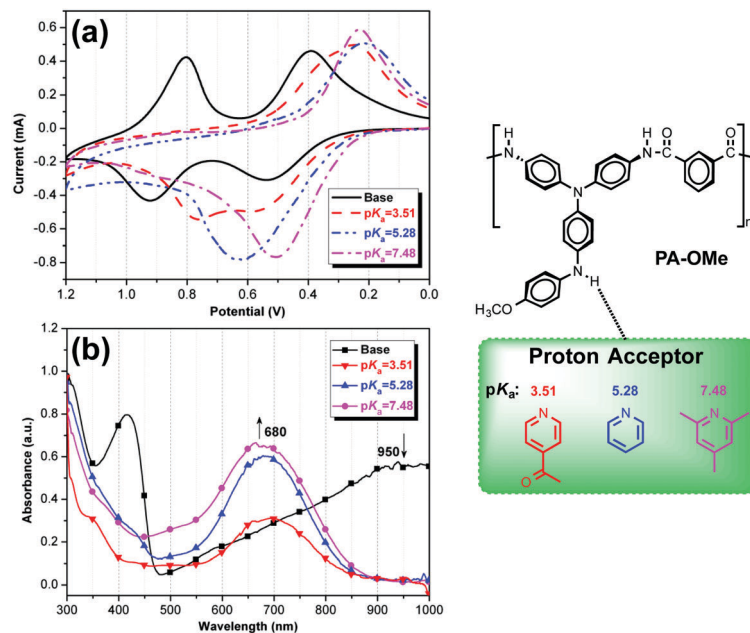
Fig. 3 (a) The shift of second potential for **PA-OMe** with different pK_a of the pyridines (36 μmol) in 0.1 M TBAP/CH$_3$CN. (b) The absorption spectra of **PA-OMe** with different pK_a of the pyridines (80 μmol) in 0.1 M TBAP/CH$_3$CN (polymer films with an area of about 0.5 cm × 1.1 cm).

the different forces between the secondary amine and pyridines. Their corresponding polyamides also have similar electrochemical behavior (Fig. 3). The CV diagrams of polyamide **PA-OMe** revealed two reversible oxidation waves at E_1^{ox} = 0.56 V and E_2^{ox} = 0.93 V, respectively (black solid line). After adding the pyridines with different pK_a, the $E_2^{ox'}$ decreased on increasing the pK_a value of the pyridines. In particular, in the presence of Me$_3$Py, the final $E_2^{ox'}$ is also lower than E_1^{ox} with the peak current around 2 times higher than that of E_1^{ox}, manifesting a similar potential inversion behavior to the structure-related compounds. Moreover, the absorption spectra change of **PA-OMe$^{+\bullet}$** after adding different pyridines is presented in Fig. 3b to illustrate the strength of H-bonding between **PA-OMe$^{+\bullet}$** and the pyridines accordingly. The disappearance of the IV-CT band at around 950 nm can be observed after each pyridine was added. Besides, the intensity of the new absorption band at around 680 nm is highly related to the pK_a of the pyridines, further providing additional support for the presence of H-bonding.

Conclusion

In summary, this work reports the synthesis of triarylamine-based high-performance polyamides with secondary amines and their electrochemical detection of pyridines characterized by potential inversion resulting from H-bonding interactions. Pyridines with different substituent and pK_a values have been manifested by the effect on electrochemical properties of the polyamides. The potential inversion could be clearly observed from the CV diagrams as Me$_3$Py is applied, which is also supported by *in situ* UV-vis absorption measurements. Thus, these results demonstrate that the triarylamine-based polymers containing secondary amines can effectively interact with proton acceptors to result in ionic hydrogen bonding, and this phenomenon can be successfully monitored using cyclic voltammogram diagrams and absorption spectra.

Acknowledgements

Notes and references

1 (*a*) R. Bao, C. Wang, L. Dong, R. Yu, K. Zhao, Z. L. Wang and C. Pan, *Adv. Funct. Mater.*, 2015, **25**, 2884; (*b*) M. M. Barsan, M. E. Ghica and C. M. A. Brett, *Anal. Chim. Acta*, 2015, **881**, 1; (*c*) S.-Y. Kuo, H.-H. Li, P.-J. Wu, C.-P. Chen, Y.-C. Huang and Y.-H. Chan, *Anal. Chem.*, 2015, **87**, 4765.

2 N. Gupta and H. Linschitz, *J. Am. Chem. Soc.*, 1997, **119**, 6384.

3 (*a*) Y. Ge, R. R. Lilienthal and D. K. Smith, *J. Am. Chem. Soc.*, 1996, **118**, 3976; (*b*) Y. Ge, L. Miller, T. Ouimet and D. K. Smith, *J. Org. Chem.*, 2000, **65**, 8831; (*c*) Y. Ge and D. K. Smith, *Anal. Chem.*, 2000, **72**, 1860; (*d*) J. Bu, N. D. Lilienthal, J. E. Woods, C. E. Nohrden, K. T. Hoang, D. Truong and D. K. Smith, *J. Am. Chem. Soc.*, 2005, **127**, 6423; (*e*) C. Chan-Leonor, S. L. Martin and D. K. Smith, *J. Org. Chem.*, 2005, **70**, 10817.

4 Y.-C. Chung, Y.-J. Tu, S.-H. Lu, W.-C. Hsu, K. Y. Chiu and Y. O. Su, *Org. lett.*, 2011, **13**, 2826.

5 (*a*) D. H. Evans and K. Hu, *J. Chem. Soc., Faraday Trans.*, 1996, **92**, 3983; (*b*) N. A. Macías-Ruvalcaba and D. H. Evans, *J. Phys. Chem. B*, 2006, **110**, 5155.

6 P. Hapiot, L. D. Kispert, V. V. Konovalov and J.-M. Savéant, *J. Am. Chem. Soc.*, 2001, **123**, 6669.

7 H. J. Yen and G. S. Liou, *Polym. Chem.*, 2012, **3**, 255.